mTOR-dependent dysregulation of autophagy contributes to the retinal ganglion cell loss in streptozotocin-induced diabetic retinopathy

Sanjar Batirovich Madrakhimov
Soonchunhyang University Hospital Bucheon
Jin Young Yang
Soonchunhyang University Hospital Bucheon
Jin Ha Kim
Soonchunhyang University Hospital Bucheon
Jung Woo Han
Soonchunhyang University Hospital Bucheon
Tae Kwann Park (tkpark@schmc.ac.kr)
Soonchunhyang University Hospital Bucheon https://orcid.org/0000-0001-9689-4384

Research

Keywords: diabetic retinopathy, neurodegeneration, autophagy, apoptosis, the mechanistic target of rapamycin (mTOR)

Posted Date: August 17th, 2020

DOI: https://doi.org/10.21203/rs.3.rs-56279/v1

Version of Record: A version of this preprint was published on February 26th, 2021. See the published version at https://doi.org/10.1186/s12964-020-00698-4.

Abstract

Background: Neurodegeneration, an early event in the pathogenesis of diabetic retinopathy (DR), precedes clinically detectable microvascular damage. Autophagy dysregulation is considered a potential cause of neuronal cell loss, however underlying mechanisms remain unclear. The mechanistic target of rapamycin (mTOR) integrates diverse environmental signals to coordinate biological processes, including autophagy. Here, we investigated the role of mTOR signaling in neuronal cell death in diabetic retinopathy.

Methods: Diabetes was induced by a single intraperitoneal injection of streptozotocin and tissue samples were harvested at 1, 2, 3, 4, and 6 months of diabetes. Early-stage of diabetic retinopathy was investigated in 1-month-diabetic mice treated with phlorizin or rapamycin. The effect of autophagy modulation on retinal ganglion cells was investigated in 3-months-diabetic mice treated with phlorizin or MHY1485. Tissue samples obtained from treated/untreated diabetic mice and age-matched controls were used for Western blot and histologic analysis.

Results: mTOR-related proteins and glucose transporter 1 (GLUT1) was upregulated at 1 month and downregulated in the following period up to 6 months. Diabetes-induced neurodegeneration was characterized by an increase of apoptotic marker – cleaved caspase 3, a decrease of the total number of cells, and NeuN immunoreactivity in the ganglion cell layer (GCL), as well as an increase of autophagic protein. Insulin-independent glycemic control restored the mTOR pathway activity and GLUT1 expression, along with a decrease of autophagic and apoptotic proteins in 3-months-diabetic mice neuroretina. However, blockade of autophagy using MHY1485 resulted in a more protective effect on ganglion cells compared with phlorizin treatment.

Conclusion: Collectively, our study describes the mechanisms of neurodegeneration through the hyperglycemia/ mTOR/ autophagy/ apoptosis pathway.

Background

Diabetic retinopathy (DR) is a severe ocular complication of diabetes mellitus (DM) leading to vision loss in adults aged 20–79 years [1, 2]. The prevalence of DR ranges from 21.7–34.6% among diabetic individuals [2–5], whose number was estimated at 451 million of adults in 2017 and is projected to increase to 693 million worldwide by 2045 [6]. Despite the introduction of various screening programs for DR detection, it remains the leading cause of blindness for 2.6 million adults among the global population [7, 8].

DR is a multifactorial disease with extremely complex mechanisms of development [9]. DR is classified into non-proliferative diabetic retinopathy and proliferative diabetic retinopathy [10, 11]. These “early” and “advanced” stages are characterized by the level of microvascular and ischemic damage of the retina, which determines visible clinical manifestations [11]. However, advances in retinal imaging techniques and electrophysiological studies demonstrated subtle functional deficits and neuronal abnormalities in

patients without background retinopathy [12–19]. Experimentally, aside from compromise of vascular cells, alterations of various retinal neuronal cells, macroglia and microglia have been shown in diabetes [20–27]. Thus, the classic view on DR as the microcirculatory pathology evolved into the concept of disease of the retinal neurovascular unit (NVU), where neurodegeneration precedes clinically detectable microvascular damage [11, 28–31].

The concept of retinal NVU describes neurons, glial, and vascular cells as a functional and structural integration, which is essential for maintaining the homeostasis in the inner retina [11, 28–30, 32]. Under diabetic conditions, such as hyperglycemia, abnormal blood flow, and others, the NVU appears to be an adaptive mechanism, which fails after prolonged metabolic perturbations [29, 31]. All components of the NVU are affected by diabetes, but which cells are primarily involved in pathologic processes remain unclear [32, 33]. Although vascular, glial, and neuronal cell damage appears to be interdependent, the latter significantly contributes to the development of DR by triggering molecular events resulting in the blood-retinal-barrier dysfunction, microangiopathy, and the proinflammatory milieu [28, 31, 33, 34]. One of the hallmarks of neuronal cell damage is persistent apoptosis, which may be initiated by several pathways, such as glutamate excitotoxicity, loss of neuroprotective factors, oxidative stress, and neuroinflammation [31, 34, 35]. However, growing evidence suggests that defective autophagy also contributes to the diabetes-induced neuronal cell death [36–39]. Autophagy is an adaptive mechanism that may be upregulated against various stress conditions, such as nutrient deprivation, oxidative stress, and others to maintain cellular homeostasis by lysosomal degradation of damaged intracellular elements, and supplying with nutrients [40–42]. However, dysregulated autophagy may have fatal consequences for the cell, indicating a complex network between autophagy and apoptosis. [40–42]. At this point, we wondered that if autophagy dysregulation involved in diabetes-induced neurodegeneration, what is the role of the mechanistic target of rapamycin (mTOR) pathway in this context, which is the master regulator of autophagy. This was a starting point of our investigation and we hypothesized how the mTOR pathway may contribute to the neuronal cell death in the DR (Fig. 1). To address the question, we studied the dynamics of events leading to the neuronal cell death in a streptozotocin(STZ)-induced mouse model of diabetes over 6 months of period. The results demonstrated that activity of the mTOR pathway was initially increased at early period of diabetes and this increase was reversed by insulin-independent glycemic control. At advanced stages of diabetes, we observed downregulation of the mTOR activity accompanying with autophagy activation and neuronal cell loss. Furthermore, the management of hyperglycemia could restore the mTOR activity, inhibit autophagy and prevent neuronal cell death. Interestingly, treatment with the mTOR activator, which is MHY1485, demonstrated a more prominent protective effect on neuronal cells even under hyperglycemic conditions. Therefore, downregulation of mTOR activity by various factors associated with prolonged hyperglycemia may be responsible for the autophagy-induced neuronal cell death in the DR. These findings have implications for the development of mTOR-based therapies to manage autophagy-related neuronal cell death in the early stages of DR.

Materials And Methods

Animal care

All animal experiment was designed and conducted in accordance with the Guide of the Care and Use of Laboratory Animals, the Association for Research in Vision and Ophthalmology Statement for the Use of Animals in Ophthalmic and Vision Research, and approved by the Institutional Animal Care and Use Committee for Soonchunhyang University Hospital Bucheon.

Mice used in this study were C57/BL6 strain (8 weeks, male, 22 ~ 24 g) and purchased from the Orient Bio Inc., (Seongnam, South Korea). All mice were housed in breeding cages in a room with a 12/12-hour light/dark cycle and had free access to food and water. The humidity and temperature were respectively maintained at 50% and 23 ~ 26℃.

Induction Of Diabetes

Diabetes was induced by a single i.p. injection of STZ (150 mg/kg; Sigma-Aldrich, St. Louis, MO, USA). STZ was freshly prepared in 100 mM citrate buffer (pH 4.5). To avoid sudden hypoglycemia post-injection, the mice were fed 10% sucrose overnight. Hyperglycemia was confirmed by measuring blood glucose using the Accu-Check active blood glucose monitor (Roche Diagnostics, Mannheim, Germany) 2 days and 2 weeks post-injection. Only mice with non-fasting blood glucose levels > 300 mg/dL, polyuria, or glucosuria were defined as STZ-induced diabetic mice and used in the experiments. Non-diabetic, age-matched mice were used as the controls. The general parameters of mice obtained on the day of the sacrifice are given in Table 1.

Grouping And Treatment Regimen

To evaluate the natural course of DR, we observed 60 mice over 6 months of period. Animals were assigned to 6 groups depending on observation period: 1) Normal control, 2) 1 m DM, 3) 2 m DM, 4) 3 m DM, 5) 4 m DM and 6) 6 m DM (Fig. 2a). The effects of short-term hyperglycemia on the retina were investigated on 40 mice, divided into 4 groups: 1) Normal control, 2) 1 m DM, 3) 1 m DM/PHL 4) 1 m DM/Rapa (Fig. 2b). Mice in the 1 m DM/PHL group received two daily subcutaneous injections of phlorizin (Cayman Chemical, Ann Arbor, MI) dissolved in 60% propylene glycol in phosphate-buffered saline at a dose of 200 mg/kg of body weight during the last 7 full days of the experiment and the morning of the 8th day, 3 h before sacrifice. Mice in the 1 m DM/Rapa group, received daily i.p. injections of rapamycin (Sigma-Aldrich, St. Louis, MO) diluted in 4% ethanol and 5% Tween-20 in distilled water at a dose of 3 mg/kg for the same period as for the 1 m DM/PHL group [43].

The effects of long-term hyperglycemia on the retina of diabetic mice were evaluated on 40 mice, divided into 4 groups: 1) Normal control, 2) 3 m DM, 3) 3 m DM/PHL, and 4) 3 m DM/MHY (Fig. 2c). Mice in the 3 m DM/PHL group received two daily subcutaneous injections of PHL during the last 10 full days of the experiment and the morning of the 11th day, 3 h before sacrifice. Mice in the 3mDM/MHY group received daily i.p. injections of MHY1485 (MedChem Express, Monmouth Junction, NJ) at a dose of 10 mg/kg for the same period as for the 3 m DM/PHL group. Eight diabetic mice died in the course of this study.

Tissue Collection And Preparation

After completing the experiment, mice were used for WB and histologic analysis. For histologic analysis, mice were deeply anesthetized and perfused intracardially with 0.1M phosphate buffer (PB) containing 1000 U/ml of heparin, followed by an infusion of 4% paraformaldehyde (PFA) in 0.1M PB. The eyecup was made by removing the anterior segment from the enucleated mouse eye and fixed with 4% paraformaldehyde (Biosesang, Seongnam, South Korea) for 1 h, dehydrated in 30% sucrose overnight, and embedded in frozen section compound (Leica Biosystems Richmond, IL). The sample collection for the WB experiment was that the neuroretina was separated from the enucleated mouse eyes, pooled together and stored at − 80 °C until the experiment.

Western Blot

Neuroretinal tissue was disrupted in RIPA II lysis buffer (Gendepot, Barker, Tx) containing Xpert phosphatase inhibitor cocktail (Gendepot, Barker, Tx) and Xpert protease inhibitor cocktail (Gendepot, Barker, Tx) for 1 h on the ice. Insoluble material was removed by centrifugation (13000 rpm, 15 min, 4 °C), and the only supernatant was obtained. Protein lysate was quantified using Pierce BCA Protein Assay kit (Thermo scientific, Middlesex, MA) according to the manufacturer's instruction.

The lysates were denatured in 4x Laemmli sample buffer (Gendepot, Barker, Tx), boiled for 10 min at 95 °C. Aliquots of each sample with an equal amount of protein were separated using SDS-acrylamide gel in the range from 6 to 10%, depending on the molecular weight of the target antibody and transferred onto polyvinylidene fluoride membrane (ATTO, Amherst, NY). The membranes were incubated with 5% skim milk in Phosphate-Buffered Saline (PBS) containing 0.1% Tween-20 for detection of total proteins and 5% BSA in PBS containing 0.1% Tween-20 for phosphorylated proteins for 1 h at room temperature and incubated with anti-mTOR, anti-phospho-S6 ribosomal protein (S240/244) from Cell signaling technology (Danvers, MA), anti-phospho-mTOR (S2448), anti-GLUT1 from Abcam (Cambridge, UK), anti-β-actin from Santa Cruz Biotechnology (Dallas, TX) antibodies overnight at 4 °C; details on antibodies are given in Supplemental Table S1. After washing, the membranes were incubated with horseradish peroxidase (HRP)-conjugated goat anti-rabbit IgG and goat anti-mouse IgG (Genedepot, Barker, Tx) at room temperature for 2 h. The immunoreactive signal was developed using Western blotting detection kit (EzWestLumi plus, ATTO Corporation, Tokyo, Japan) and read with Azure Biosystems™ c280 (Azure Biosystems, Dublin, CA, USA). Bands on blots were quantified using the ImageJ software (National Institutes of Health, Bethesda, MD).

Immunofluorescence

Fresh eyecup cryosections (10 μm in thickness) were made with a Cryotome (Thermo Fisher Scientific Shandon Cryotome, Middlesex, MA). The slides were washed with 1xPBS containing 0.1% Triton X-100 (Sigma-Aldrich, St. Louis, MO) and blocked with 5% donkey serum in PBST for 1 h. The blocked slides were then incubated with anti-phospho-mTOR (S2448), anti-GLUT1 from Abcam (Cambridge, UK), anti-phospho-S6 ribosomal protein (S240/244) and anti-GFAP (CST) from Cell signaling technology (Danvers, MA), anti-Glutamine synthetase from Millipore (Billerica, MA), anti-NeuN from Millipore (Billerica, MA), anti Calbindin from Sigma-Aldrich (St. Louis, MO), anti-Cleaved caspase-3 from Cell signaling technology

(Danvers, MA), anti-Beclin1 from Novus Biologicals (Littleton, CO) antibodies for 2 h and detected with secondary antibodies (Alexa Fluor 488 or 568 or 647, dilution 1:1000; Invitrogen Corp., Carlsbad, CA); details on antibodies are given in Supplemental Table S1. Nuclear counterstaining was performed with Hoechst 33342 (Invitrogen Corp, Carlsbad, CA). After washing, the sections were mounted with fluorescence mounting medium (Dako, Santa Clara, CA).

Image Analysis And Cell Counting

All slides were imaged using a Leica SP8 (Leica Microsystems, Wetzlar, Germany) confocal microscope. Cleaved caspase-3, NeuN and Hoechst positive cells (n = 6 per group) were manually calculated using Image J software (National Institutes of Health, Bethesda, MD).

String Analysis

The potential interactions among selected proteins were analyzed using free online database of currently known proteins – STRING (Search Tool for the Retrieval of Interacting Genes, v11.0). IDs of selected proteins were used as an input in the database (http://string-db.org/) to find functional associations in homo sapiens and mus musculus with a minimum interaction score of 0.400 (medium confidence). Active interaction sources included text mining, experiments, databases, gene fusion, co-occurrence, co-expression, and neighborhood.

Statistical analysis

Data are expressed as means ± standard deviation. Differences among groups were analyzed using the Mann-Whitney U test. Differences were considered statistically significant when $P \leq 0.05$.

Results

Hyperglycemia-induced molecular events and consequences in STZ mouse retina.

We observed the effect of hyperglycemia on the expression of mTOR related proteins and GLUT1 for 6 months after induction of diabetes. After 1 month of STZ injection, pmTOR (S2448) and its downstream effector – pS6 (S240/244) levels were upregulated followed by substantial decrease at 2, 3 and 4 months. Six months samples demonstrated the lowest level of pmTOR (S2448) and pS6 expression (Fig. 3A, B). GLUT1 also showed higher levels at one month after diabetes induction, and then gradually decreased by 6 months of observation (Fig. 3A, B).

To evaluate neuronal cell death in the diabetic retina, we immunostained the cryosections of the retina of STZ mice at 1, 3, 6 months for Cleaved caspase-3 and NeuN, normal mouse retina served as control (Fig. 3C). Cleaved caspase-3 signals were detected in the ganglion cell layer (GCL) of the diabetic retina, which was weak at 1 month and strong at 3 and 6 months (Fig. 3C), positive signal was not observed in normal retina. Counting of Cleaved caspase-3-positive cells demonstrated a gradual increase of apoptotic cell number and a peak after 6 months of diabetes induction ($p < 0.05$, Fig. 3D). In addition, NeuN

immunoreactivity of ganglion cells progressively decreased at 3 and 6 months, which was also confirmed by counting of NeuN-positive cells ($p < 0.05$) (Fig. 3C and 3E). The total number of cells in GCL was also decreased after 3 ($p > 0.05$) and 6 months of diabetes ($p < 0.05$) (Fig. 3E).

pmTOR S2448, pS6 and GLUT1 expressing cells in the normal mouse retina.

Next, we performed immunofluorescence assay to identify pmTOR S2448, pS6 and GLUT1 expressing cells in the neuroretina of normal mouse. pmTOR S2448 is expressed in the GCL, in both plexiform layers and the cell bodies in the inner nuclear layer (INL), as was found to be the similar for GLUT1, which was also expressed in the cell bodies of the outer nuclear layer (ONL) (Fig. 4a). Co-immunostaining of pmTOR S2448 and NeuN confirmed the expression of activated mTORC1 in ganglion cells (Fig. 4b). Phosphorylated mTOR at S2448 was also expressed in Calbindin positive cells (Fig. 4c). Moreover, pmTOR S2448 is expressed in the endfeet and cell bodies of Müller cells immunostained for Glutamine synthetase (GS, Fig. 4d), which was also co-localized with GLUT1 (Fig. 4e).

The downstream effector of mTORC1 complex, pS6, was found to be expressed highly in the GCL and the outermost part of the INL, weakly in the cell bodies in the inner half of the INL. While the source of the pS6 signal in the GCL was NeuN-positive ganglion cells (Fig. 4f), signals from the outermost part of the INL originated from the cell bodies and processes of horizontal cells immunostained for Calbindin (Fig. 4g). Weak pS6 signal colocalized with NeuN positive cells in the inner nuclear layer, which are likely to be amacrine cells or ectopic ganglion cells (Fig. 4f).

Dynamics of hyperglycemia-induced pS6 and GLUT1 expression in STZ mouse retina.

After 1 month of hyperglycemia, we observed upregulation of pS6 expression in the inner retina. After 3 months of hyperglycemia, pS6 expression was downregulated, amacrine cells and processes of horizontal cells lacked pS6, while cell bodies of ganglion cells and horizontal cells retained pS6 expression. A few pS6-positive ganglion cells and horizontal cells were observed after 6 months of diabetes (Fig. 5). GLUT1 expression was also increased at 1 month of diabetes and was gradually decreased evenly in the neuroretina at 3 and 6 months of diabetes (Fig. 5).

Hyperglycemia-induced activation of glia and autophagy dysregulation in STZ-mouse retina.

Glia reactivity was detected by immunostaining of cryosections of normal and 3 m STZ mouse retina with antibody against glial fibrillary acidic protein (GFAP). In normal mouse retina, GFAP expression was limited to the astrocytes and Müller cell endfeet in the nerve fiber layer (NFL) and GCL (Fig. 6C), whereas in the 3 m DM mouse retina, GFAP expression was elevated and extended to the glia in the NFL, GCL and IPL (Fig. 6D). Moreover, in the 3 m DM mouse retina, pmTOR S2448 expression was evenly downregulated comparing to those of the normal mouse retina (Fig. 6C and 6D).

To evaluate autophagy flux, we immunostained cryosections of normal and 3 m STZ-mouse retina for Beclin1. In the normal mouse retina, Beclin1 expression which was detected in the GCL, INL and OPL in

the normal mouse retina. Beclin1 immunoreactivity in 3 m STZ mouse retina was clearly upregulated and extended to the IPL, ONL and photoreceptor cell layer (Fig. 6A and 6B).

The effects of short-term hyperglycemia on STZ-mouse retina are reversible by glycemic control.

pmTOR S2448 expression was upregulated at 1 month of diabetes and phlorizin (PHL) treatment demonstrated similar levels as those of normal mouse neuroretina demonstrated by Western Blot and immunofluorescence assay. Hyperglycemia-induced upregulation of pS6, as well as GLUT1 levels, were also decreased by glycemic control with PHL treatment. As expected from mTOR inhibition, rapamycin treatment resulted in decreased expression of pmTOR S2448 and pS6 levels, but we also observed downregulation of GLUT1 (Fig. 7A and 7B).

Glial response was monitored by immunofluorescence assay. In the normal mouse retina, GFAP expression was confined to astrocytes in the NFL and GCL, whereas in the 1 m DM retina, astrocytes located in the inner plexiform layer (IPL) were also stained along with rare Müller glia resembling GFAP positive cells. PHL and rapamycin treatment returned the levels of GFAP expression back to the normal state (Fig. 7C).

Autophagy dysregulation contributes to neuronal damage after long-term hyperglycemia.

pmTOR S2448 and pS6 expression was decreased at 3 month of diabetes and PHL treatment recovered mTOR activity in the neuroretina as demonstrated by Western Blot and immunofluorescence assay (Fig. 8A and 8G). GLUT1 expression in the neuroretina of 3 m STZ-mouse was also increased following PHL treatment (Fig. 8A). MHY1485 treatment successfully activated mTOR in the neuroretina of 3 m STZ-mouse, since pmTOR S2448 level detected by WB and immunofluorescence assay, was high.

Beclin1 immunoreactivity in the retina from 3 m DM/PHL group resembled the similar expression pattern as those of normal control group: immunofluorescence signal was detected in the GCL, INL, and OPL. However, MHY1485 treatment resulted in stronger inhibition of autophagy, since Beclin1 signal was observed only in the GCL (Fig. 8B). Calbindin staining did not reveal any difference in OPL of the retina from all groups; meanwhile, the GCL differed between all experimental groups (Fig. 8B and 8C).

To assess, how autophagy affects the neuronal cells in the GCL, we immunostained the retinal tissues from 3mDM, 3mDM/PHL and 3mDM/MHY groups for Cleaved caspase 3 and NeuN, retinal tissues from normal mouse served as control. We observed a clear increase in Cleaved caspase 3 labeling in the GCL of 3 m STZ mouse, indicating high apoptotic activity after long-term hyperglycemia (Fig. 8D). PHL treatment resulted in moderate decrease of immunoreactivity and number of Cleaved caspase 3 positive cells (Fig. 8D and 8E). However, autophagy blocking with mTOR activator resulted in significant decrease of immunoreactivity and number of Cleaved caspase 3 positive cells comparing to those of 3 m DM and 3 m DM/PHL groups (Fig. 8D and 8E). Quantification of neuronal cells in the GCL of tissues from treatment groups also confirmed the neuronal cells rescue from apoptotic activity induced by long-term hyperglycemia (Fig. 8F). The total number of cells in GCL was decreased in the retinal tissues from

3mDM group comparing to those of from the normal group and 3mDM/PHL demonstrated a similar amount of Hoechst positive cells ($p > 0.05$). However, NeuN positive cell number was higher in tissues from 3mDM/PHL group comparing to 3mDM group ($p > 0.05$). In the tissues of the 3mDM/MHY group, total number of cells and NeuN positive cell was the highest among STZ-injected groups ($p < 0.05$) (Fig. 8F).

To confirm the neuronal rescue following autophagy modulation, we studied the glial response by GFAP labeling (Fig. 8G). GFAP positive astrocytes and Müller glia resembling cells were detected in the NFL, GCL, and IPL of 3 m STZ-mouse. MHY1485 treated mouse retina demonstrated GFAP signals only in the NFL and GCL as demonstrated normal mouse retina. Similar results were found in those of PHL-treated mice (Fig. 8G).

Discussion

The major contributor to the development of DR is the high levels of glucose in the blood [1, 44]. Glucose – the primary energy source of the cell – is a polarized large molecule, which cannot traverse the cell membrane by diffusion. In the retina, the proteins of facilitated diffusion glucose transporter family are proposed to be responsible for glucose transportation [45]. Among others, glucose transporter 1 (GLUT1) is the most studied and considered as the major transporter in the neural retina and blood-retinal barrier (BRB). [45–50]. As being insulin-independent glucose transporter, the GLUT1 expression and transport activity can be stimulated by the levels of glucose in the blood [51, 52]. Under diabetic conditions, hyperglycemia results in an increase of intracellular glucose concentration in the neural retina potentially through hyperglycemia-induced GLUT1 upregulation as an adaptive response [53–55]. However, long-term hyperglycemia may lead to the downregulation of GLUT1 in the retina [56–58]. Differential expression of GLUT1 depending on clinical stages of DR was also observed in postmortem human retina [46, 59, 60]. In the inner BRB, focal upregulation of GLUT1 expression was observed in long-standing DM patients with minimal or no clinical retinopathy [59]. However, GLUT1 expression was significantly decreased in human eyes with clinically evident DR [60]. Another study reported that GLUT1 immunoreactivity was not even observed in the neovascular tissue of patients with proliferative DR, which is an advanced stage [46]. Several mechanisms of GLUT1 downregulation are implicated upon long-term hyperglycemia including oxidative stress signaling and accumulation of advanced glycation end-products (AGEs) and their precursors, such as methylglyoxal, which, inter alia, may inhibit expression of the glucose transporter genes [61–64]. Also, growing data suggests another detrimental effect of long-term hyperglycemia on the retina which is manifested in the generation of autophagy processes through nutrient stress, oxidative stress, endoplasmic reticulum stress, hypoxia, inflammation, and others [39, 41, 65]. At this point, we hypothesized that the mTOR signaling pathway may be the link between the factors related to hyperglycemia and autophagy, consequently leading to the neuronal cell loss in DR (Fig. 1).

mTOR is atypical serine/threonine protein kinase from the phosphoinositide 3-kinase (PI3K)-related kinase family, which maintains the balance between anabolic and catabolic processes in response to a variety of physiological and pathological conditions [66]. mTOR pathway regulates myriad biological

processes such as protein synthesis, proliferation, autophagy, metabolism, cell survival, and others through distinct protein complexes including mTOR complex 1 (mTORC1), mTOR complex 2 (mTORC2) and mTOR complex 3 (mTORC3) [66, 67]. The most intensively studied of all mTOR complexes is undoubtedly mTORC1. mTORC1 senses the main intracellular and extracellular signals, which are nutrient levels, growth factors, oxygen, amino acids, and stress, to regulate variety of essential metabolic processes, such as protein synthesis and autophagy [66].

High levels of nutrients, such as intracellular hyperglycemia directly or indirectly activates mTORC1 resulting in increased anabolism [66, 68]. In vitro experiments demonstrated that increased extracellular glucose stimulates GLUT1 expression and mTORC1 pathway, moreover, adenoviral overexpression of GLUT1 had similar effect on the latter [69]. Another study demonstrated that knockdown or inhibition of GLUT1 decreases retinal glucose, superoxide radicals and vascular endothelial growth factor in the early period of diabetes [70]. Activation of mTORC1 pathway in the early period of diabetes (28 days) has previously been reported in the retina of STZ-induced rat model [71]. In our study, 6 months monitoring of STZ-diabetic mice revealed biphasic expression of mTORC1 pathway proteins, demonstrating upregulation at 1 month and decreased expression in the following period (Fig. 3A-B). Of note, the upregulation of mTOR activity followed by downregulation has been reported in the other tissues of STZ-induced diabetes models, but the follow-up period lasted only 6 weeks [72]. The biphasic pattern was also observed in GLUT1 expression and activation of mTORC1 pathway correlated with the time point of enhanced expression of GLUT1 (Fig. 3A-B). Thus, activation of the mTOR pathway in the retina of STZ-induced diabetic mice is likely to be in response to hyperglycemia-induced GLUT1 upregulation leading to the increased glucose uptake. These findings have been confirmed by further experiments, where insulin independent glycemic control via PHL treatment resulted in downregulation of mTORC1, pS6 and GLUT1 proteins (Fig. 7A-7B). PHL, a natural metabolite isolated from the plants, improves the hyperglycemia by preventing renal glucose resorption and intestinal glucose absorption through suppression of the sodium–glucose transporters [73]. Previous studies demonstrated the protective effect of PHL on the retina from diabetes by decreasing of blood glucose level [74, 75], which was also observed in our study (Fig. 2, Table 1).

There is no consensus regarding the vascular or neural damage is the earliest morphological consequence of hyperglycemia in the diabetic retina. Nevertheless, the “feed-forward” concept suggests that neuronal dysfunction eventually compromises the overall integrity of the NVU, leading to neurodegeneration and vascular damage [33, 76]. Neurodegeneration is characterized by a decreased thickness of retinal nerve fiber layer, loss of ganglion cells and different types of amacrine cells [19, 20, 24, 26]. Neuronal cell loss was observed as early as after 1 month of STZ-induced diabetes [26]. Apoptosis is proposed to be the main degenerative mechanism in DR [34]. Therefore, we evaluated the immunoreactivity of cleaved caspase 3 in the diabetic retina, which was gradually increased in the GCL over the follow-up period in line with the results of other studies (Fig. 3C, 3D) [27]. The reduction of NeuN immunoreactivity and the total number of cells in the GCL also indicated hyperglycemia-induced neuronal cell damage (Fig. 3C, 3E), mirroring the results of previous studies [26]. We assume that there may be a functional relationship between the expression of ribosomal protein S6 in the GCL and reduced

immunoreactivity of NeuN in the diabetic retina (Fig. 4f), since pS6 is one of the downstream effector of mTORC1 pathway on protein synthesis and the part of translational machinery [77]. Further studies are needed to evaluate the significance of neuronal expression of pS6 in the context of neurodegeneration in DR.

One chain of pathological processes triggered by hyperglycemia-related conditions is autophagy, which may cause neurodegeneration in DR [41]. In vitro experiments demonstrated that autophagy strongly depends on the deactivation of the mTORC1 pathway which could be caused by various factors including energy deprivation and hypoxia in terms of the pathogenesis of DR [41, 65, 78]. Inhibition of the mTORC1 pathway initiates the cascades of events leading to the increased expression of autophagic proteins, including LC3B and Beclin1 [65]. Beclin1 is recruited during the early phases of degradative autophagy flux and its upregulation was found to contribute to the initial deregulation of autophagy in human diabetic retinas as well as in STZ-induced diabetes models [36, 38, 79]. To the best of our knowledge, there currently exists no report regarding the involvement of the mTOR pathway in autophagy-induced ganglion cell loss in DR (Supplemental Fig.S1). In our study, upregulation of Beclin1 in the entire inner retina was accompanied with the signs of neuronal cell damage, such as activation of apoptotic marker – cleaved caspase 3 and decrease of the total number of cells in the GCL, along with depleted NeuN immunoreactivity in ganglion cells (Fig. 6B; Fig. 8C-8G). PHL treatment confirmed that hyperglycemia-induced autophagy deregulation is responsible for neuronal cell loss and mTORC1 pathway activity is required to preserve neurons in DR (Fig. 8). The number of apoptotic cells was decreased and NeuN immunoreactivity was higher in the GCL of PHL-treated mice retina comparing to that of 3 m diabetic control mice (Fig. 8C-8G). However, blockade of autophagy by mTOR activator – MHY1485 injections resulted in the more prominent rescue of neuronal cells, as apoptotic cell number in the GCL was the lowest among retinas of all diabetic groups (Fig. 8E). In addition, the total number of cells as well as NeuN positive cells in MHY1485 treated retina was higher than retinas from other diabetic groups (Fig. 8F-G). The less beneficial effect of glycemic control on the ganglion cells comparing to autophagy blockade is likely due to cumulatively inhibition of the mTORC1 pathway by hyperglycemia-related conditions, consequently results in autophagy dysregulation in the diabetic retina. As a result, glycemic control could not fully resolve ganglion cell death in DR (Fig. 8D-F). Moreover, the fact that glycemic control could not restore mTORC1 pathway activity, as we observed in the MHY1485 treated mouse retina, supports this assumption (Fig. 8A). These findings suggest that mTOR pathway plays a crucial role in neurodegeneration promoted by diabetes and modulation of mTORC1 activity has the rescue effect on the retina through inhibition of autophagy even in uncontrolled hyperglycemia conditions (Fig. 9).

Conclusion

Our study suggests that during the early period of diabetes, hyperglycemia-induced GLUT1 activation results in increased glucose uptake and mTORC1 signaling activity. However, long-term hyperglycemia-related conditions cause mTOR inhibition leading to autophagy dysregulation, hence the reason for the neuronal cell death in DR. Thus, the current study not only describes the mechanisms of

neurodegeneration through hyperglycemia-/mTOR/autophagy/apoptosis pathway, but also provides a rationale for the development of new strategies based on autophagy modulation to manage neuronal cell death in the early period of DR.

Abbreviations

AGEs: advanced glycation end-products; BRB: blood-retinal barrier; DM: Diabetes mellitus; DR: Diabetic retinopathy; GCL: ganglion cell layer; GFAP: glial fibrillary acidic protein; GLUT1: glucose transporter 1; GS: Glutamine synthetase; INL: inner nuclear layer; IPL: inner plexiform layer; mTOR: mechanistic target of rapamycin; NFL: nerve fiber layer; NVU: neurovascular unit; ONL: outer nuclear layer; PB: phosphate buffer; PBS: Phosphate-Buffered Saline; PFA: paraformaldehyde; PHL: phlorizin

Declarations

Availability of data and materials

The datasets used and/or analyzed during the current study are available from the corresponding author on reasonable request.

Conflict of interest

The authors declare no competing interests.

Ethics approval

All animal experiment was designed and conducted in accordance with the Guide of the Care and Use of Laboratory Animals, the Association for Research in Vision and Ophthalmology Statement for the Use of Animals in Ophthalmic and Vision Research, and approved by the Institutional Animal Care and Use Committee for Soonchunhyang University Hospital Bucheon (SCHBC-animal-2017-04).

Funding

This research was supported by Basic Science Research Program through the National Research Foundation of Korea (NRF) funded by the Ministry of Science and ICT (grant number: 2019R1A2C1005055) and partially supported by the Soonchunhyang University research fund.

Author contributions

Conceptualization, P.T.K. and M.S.B.; Methodology, P.T.K. and M.S.B.; Validation, P.T.K. and M.S.B.; Formal analysis, M.S.B. and Y.J.Y.; Investigation, M.S.B., Y.J.Y., K.J.H. and H.J.W.; Resources, P.T.K.; Writing – Original Draft, M.S.B.; Writing – Review & Editing, P.T.K., M.S.B., and K.J.H.; Visualization, M.S.B., Y.J.Y., K.J.H. and H.J.W.; Supervision, P.T.K. and M.S.B.; Project Administration, P.T.K.; Funding Acquisition, P.T.K. All authors read and approved the final manuscript.

Acknowledgments

Not applicable.

References

1. Cheung N, Mitchell P, Wong TY. Diabetic retinopathy. *Lancet*. 2010;376(9735):124-136. doi:10.1016/S0140-6736(09)62124-3
2. Yau JWY, Rogers SL, Kawasaki R, et al. Global prevalence and major risk factors of diabetic retinopathy. *Diabetes Care*. 2012;35(3):556-564. doi:10.2337/dc11-1909
3. Zhang X, Saaddine JB, Chou CF, et al. Prevalence of diabetic retinopathy in the United States, 2005-2008. *JAMA - J Am Med Assoc*. 2010;304(6):649-656. doi:10.1001/jama.2010.1111
4. Gadkari SS, Maskati QB, Nayak BK. Prevalence of diabetic retinopathy in India: The All India Ophthalmological Society Diabetic Retinopathy Eye Screening Study 2014. *Indian J Ophthalmol*. 2016;64(1):38-44. doi:10.4103/0301-4738.178144
5. Thomas RL, Dunstan FD, Luzio SD, et al. Prevalence of diabetic retinopathy within a national diabetic retinopathy screening service. *Br J Ophthalmol*. 2015;99(1):64-68. doi:10.1136/bjophthalmol-2013-304017
6. Cho NH, Shaw JE, Karuranga S, et al. IDF Diabetes Atlas: Global estimates of diabetes prevalence for 2017 and projections for 2045. *Diabetes Res Clin Pract*. 2018;138:271-281. doi:10.1016/j.diabres.2018.02.023
7. Ting DSW, Cheung GCM, Wong TY. Diabetic retinopathy: global prevalence, major risk factors, screening practices and public health challenges: a review. *Clin Exp Ophthalmol*. 2016;44(4):260-277. doi:10.1111/ceo.12696
8. Flaxman SR, Bourne RRA, Resnikoff S, et al. Global causes of blindness and distance vision impairment 1990–2020: a systematic review and meta-analysis. *Lancet Glob Heal*. 2017;5(12):e1221-e1234. doi:10.1016/S2214-109X(17)30393-5
9. Bandello F, Lattanzio R, Zucchiatti I, Del Turco C. Pathophysiology and treatment of diabetic retinopathy. *Acta Diabetol*. 2013;50(1):1-20. doi:10.1007/s00592-012-0449-3
10. Wu L, Fernandez-Loaiza P, Sauma J, Hernandez-Bogantes E, Masis M. Classification of diabetic retinopathy and diabetic macular edema. *World J Diabetes*. 2013;4(6):290. doi:10.4239/wjd.v4.i6.290
11. Stitt AW, Curtis TM, Chen M, et al. The progress in understanding and treatment of diabetic retinopathy. *Prog Retin Eye Res*. 2016;51:156-186. doi:10.1016/j.preteyeres.2015.08.001
12. Cole ED, Novais EA, Louzada RN, Waheed NK. Contemporary retinal imaging techniques in diabetic retinopathy: a review. *Clin Exp Ophthalmol*. 2016;44(4):289-299. doi:10.1111/ceo.12711
13. Tavares Ferreira J, Alves M, Dias-Santos A, et al. Retinal neurodegeneration in diabetic patients without diabetic retinopathy. *Investig Ophthalmol Vis Sci*. 2016;57(14):6455-6460.

doi:10.1167/iovs.16-20215

14. Jackson GR, Barber AJ. Visual dysfunction associated with diabetic retinopathy. *Curr Diab Rep*. 2010;10(5):380-384. doi:10.1007/s11892-010-0132-4
15. Han Y, Adams AJ, Bearse MA, Schneck ME. Multifocal electroretinogram and short-wavelength automated perimetry measures in diabetic eyes with little or no retinopathy. *Arch Ophthalmol*. 2004;122(12):1809-1815. doi:10.1001/archopht.122.12.1809
16. Harrison WW, Bearse MA, Ng JS, et al. Multifocal electroretinograms predict onset of diabetic retinopathy in adult patients with diabetes. *Investig Ophthalmol Vis Sci*. 2011;52(2):772-777. doi:10.1167/iovs.10-5931
17. Lecleire-Collet A, Audo I, Aout M, et al. Evaluation of retinal function and flicker light-induced retinal vascular response in normotensive patients with diabetes without retinopathy. *Investig Ophthalmol Vis Sci*. 2011;52(6):2861-2867. doi:10.1167/iovs.10-5960
18. Verma A, Raman R, Vaitheeswaran K, et al. Does neuronal damage precede vascular damage in subjects with type 2 diabetes mellitus and having no clinical diabetic retinopathy? *Ophthalmic Res*. 2012;47(4):202-207. doi:10.1159/000333220
19. Vujosevic S, Midena E. Retinal layers changes in human preclinical and early clinical diabetic retinopathy support early retinal neuronal and müller cells alterations. *J Diabetes Res*. 2013;2013:905058. doi:10.1155/2013/905058
20. Barber AJ, Lieth E, Khin SA, Antonetti DA, Buchanan AG, Gardner TW. Neural apoptosis in the retina during experimental and human diabetes: Early onset and effect of insulin. *J Clin Invest*. 1998;102(4):783-791. doi:10.1172/JCI2425
21. Carrasco E, Hernandez C, Miralles A, et al. Lower Somatostatin Expression Is an Early Event in Diabetic Retinopathy and Is. *Diabetes Care*. 2007;30(11):2902-2908. doi:10.2337/dc07-0332.Additional
22. Kusari J, Zhou S, Padillo E, Clarke KG, Gil DW. Effect of memantine on neuroretinal function and retinal vascular changes of streptozotocin-induced diabetic rats. *Investig Ophthalmol Vis Sci*. 2007;48(11):5152-5159. doi:10.1167/iovs.07-0427
23. Aung MH, na Park H, Han MK, et al. Dopamine deficiency contributes to early visual dysfunction in a rodent model of type 1 diabetes. *J Neurosci*. 2014;34(3):726-736. doi:10.1523/JNEUROSCI.3483-13.2014
24. Gastinger MJ, Singh RSJ, Barber AJ. Loss of Cholinergic and Dopaminergic Amacrine Cells in Streptozotocin-Diabetic Rat and Ins2 ^{Akita} -Diabetic Mouse Retinas. *Investig Opthalmology Vis Sci*. 2006;47(7):3143. doi:10.1167/iovs.05-1376
25. Rungger-Brändle E, Dosso AA, Leuenberger PM. Glial reactivity, an early feature of diabetic retinopathy. *Investig Ophthalmol Vis Sci*. 2000;41(7):1971-1980.
26. Zeng XX, Ng YK, Ling EA. Neuronal and microglial response in the retina of streptozotocin-induced diabetic rats. *Vis Neurosci*. 2000;17(3):463-471. doi:10.1017/S0952523800173122

27. Sasaki M, Ozawa Y, Kurihara T, et al. Neurodegenerative influence of oxidative stress in the retina of a murine model of diabetes. *Diabetologia*. 2010;53(5):971-979. doi:10.1007/s00125-009-1655-6
28. Duh EJ, Sun JK, Stitt AW. Diabetic retinopathy: current understanding, mechanisms, and treatment strategies. *JCI insight*. 2017;2(14). doi:10.1172/jci.insight.93751
29. Abcouwer SF, Gardner TW. Diabetic retinopathy: loss of neuroretinal adaptation to the diabetic metabolic environment. *Ann N Y Acad Sci*. 2014;1311:174-190. doi:10.1111/nyas.12412
30. Simó R, Hernández C. Novel approaches for treating diabetic retinopathy based on recent pathogenic evidence. *Prog Retin Eye Res*. 2015;48:160-180. doi:10.1016/j.preteyeres.2015.04.003
31. Simó R, Stitt AW, Gardner TW. Neurodegeneration in diabetic retinopathy: does it really matter? *Diabetologia*. 2018;61(9):1902-1912. doi:10.1007/s00125-018-4692-1
32. Gardner TW, Davila JR. The neurovascular unit and the pathophysiologic basis of diabetic retinopathy. *Graefe's Arch Clin Exp Ophthalmol*. 2017;255(1):1-6. doi:10.1007/s00417-016-3548-y
33. Antonetti DA, Barber AJ, Bronson SK, et al. Diabetic retinopathy: Seeing beyond glucose-induced microvascular disease. *Diabetes*. 2006;55(9):2401-2411. doi:10.2337/db05-1635
34. Barber AJ, Gardner TW, Abcouwer SF. The significance of vascular and neural apoptosis to the pathology of diabetic retinopathy. *Investig Ophthalmol Vis Sci*. 2011;52(2):1156-1163. doi:10.1167/iovs.10-6293
35. Simó R, Hernández C. Neurodegeneration is an early event in diabetic retinopathy: Therapeutic implications. *Br J Ophthalmol*. 2012;96(10):1285-1290. doi:10.1136/bjophthalmol-2012-302005
36. Piano I, Novelli E, Della Santina L, Strettoi E, Cervetto L, Gargini C. Involvement of autophagic pathway in the progression of retinal degeneration in a mouse model of diabetes. *Front Cell Neurosci*. 2016;10(FEB):42. doi:10.3389/fncel.2016.00042
37. Park H-YL, Kim JH, Park CK. Different contributions of autophagy to retinal ganglion cell death in the diabetic and glaucomatous retinas. *Sci Rep*. 2018;8(1):13321. doi:10.1038/s41598-018-30165-7
38. De Faria JMLJBL, Duarte DA, Montemurro C, et al. Defective autophagy in diabetic retinopathy. *Investig Ophthalmol Vis Sci*. 2016;57(10):4356-4366. doi:10.1167/iovs.16-19197
39. Lin WJ, Kuang HY. Oxidative stress induces autophagy in response to multiple noxious stimuli in retinal ganglion cells. *Autophagy*. 2014;10(10):1692-1701. doi:10.4161/auto.36076
40. Jung HS, Lee MS. Role of autophagy in diabetes and mitochondria. In: *Annals of the New York Academy of Sciences*. Vol 1201. Blackwell Publishing Inc.; 2010:79-83. doi:10.1111/j.1749-6632.2010.05614.x
41. Rosa M Di, Distefano G, Gagliano C, Rusciano D, Malaguarnera L. Autophagy in Diabetic Retinopathy. *Curr Neuropharmacol*. 2016;14(8):810-825. doi:10.2174/1570159X14666160321122900
42. Saha S, Panigrahi DP, Patil S, Bhutia SK. Autophagy in health and disease: A comprehensive review. *Biomed Pharmacother*. 2018;104:485-495. doi:10.1016/j.biopha.2018.05.007

43. Yang JY, Madrakhimov SB, Ahn DH, et al. mTORC1 and mTORC2 are differentially engaged in the development of laser-induced CNV. *Cell Commun Signal*. 2019;17(1):64. doi:10.1186/s12964-019-0380-0
44. Jampol LM, Glassman AR, Sun J. Evaluation and Care of Patients with Diabetic Retinopathy. Ingelfinger JR, ed. *N Engl J Med*. 2020;382(17):1629-1637. doi:10.1056/NEJMra1909637
45. Kumagai AK. Glucose transport in brain and retina: Implications in the management and complications of diabetes. *Diabetes Metab Res Rev*. 1999;15(4):261-273. doi:10.1002/(SICI)1520-7560(199907/08)15:4<261::AID-DMRR43>3.0.CO;2-Z
46. Kumagai AK, Glasgow BJ, Pardridge WM. GLUT1 glucose transporter expression in the diabetic and nondiabetic human eye. *Investig Ophthalmol Vis Sci*. 1994;35(6):2887-2894.
47. Takata K, Kasahara T, Kasahara M, Ezaki O, Hirano H. Ultracytochemical localization of the erythrocyte/HepG2-type glucose transporter (GLUT1) in cells of the blood-retinal barrier in the rat. *Investig Ophthalmol Vis Sci*. 1992;33(2):377-383.
48. Gospe SM, Baker SA, Arshavsky VY. Facilitative glucose transporter Glut1 is actively excluded from rod outer segments. *J Cell Sci*. 2010;123(Pt 21):3639-3644. doi:10.1242/jcs.072389
49. Mantych GJ, Hageman GS, Devaskar SU. Characterization of glucose transporter isoforms in the adult and developing human eye. *Endocrinology*. 1993;133(2):600-607. doi:10.1210/endo.133.2.8344201
50. Thorens B, Mueckler M. Glucose transporters in the 21st Century. *Am J Physiol - Endocrinol Metab*. 2010;298(2). doi:10.1152/ajpendo.00712.2009
51. Calado SM, Alves LS, Simão S, Silva GA. GLUT1 activity contributes to the impairment of PEDF secretion by the RPE. *Mol Vis*. 2016;22:761-770. http://www.ncbi.nlm.nih.gov/pubmed/27440994. Accessed June 26, 2019.
52. Cloherty EK, Diamond DL, Heard KS, Carruthers A. Regulation of GLUT1-mediated sugar transport by an antiport/uniport switch mechanism. *Biochemistry*. 1996;35(40):13231-13239. doi:10.1021/bi961208t
53. Adachi-Uehara N, Kato M, Nimura Y, et al. Up-regulation of genes for oxidative phosphorylation and protein turnover in diabetic mouse retina. *Exp Eye Res*. 2006;83(4):849-857. doi:10.1016/j.exer.2006.04.012
54. Nyengaard JR, Ido Y, Kilo C, Williamson JR. Interactions Between Diabetes and Hypoxia Retinopathy 2004. Implications for Diabetic Retinopathy. *Diabetes*. 2004;53:2931-2938.
55. Imai H, Singh RSJ, Fort PE, Gardner TW. Neuroprotection for diabetic retinopathy. *Dev Ophthalmol*. 2009;44:56-68. doi:10.1159/000223946
56. Fernandes R, Suzuki K ichi, Kumagai AK. Inner blood-retinal barrier GLUT1 in long-term diabetic rats: An immunogold electron microscopic study. *Investig Ophthalmol Vis Sci*. 2003;44(7):3150-3154. doi:10.1167/iovs.02-1284
57. Fernandes R, Carvalho AL, Kumagai A, et al. Downregulation of retinal GLUT1 in diabetes by ubiquitinylation. *Mol vision*. 2004;10:618-628. https://eg.uc.pt/handle/10316/12771.

58. Badr GA, Tang J, Ismail-Beigi F, Kern TS. Diabetes downregulates GLUT1 expression in the retina and its microvessels but not in the cerebral cortex or its microvessels. *Diabetes*. 2000;49(6):1016-1021. doi:10.2337/diabetes.49.6.1016
59. Kumagai AK, Vinores SA, Pardridge WM. Pathological upregulation of inner blood-retinal barrier Glut1 glucose transporter expression in diabetes mellitus. *Brain Res*. 1996;706(2):313-317. doi:10.1016/0006-8993(95)01335-0
60. Tang J, Mohr S, Du YP, Kern TS. Non-uniform distribution of lesions and biochemical abnormalities within the retina of diabetic humans. *Curr Eye Res*. 2003;27(1):7-13. doi:10.1076/ceyr.27.2.7.15455
61. Roy A, Hashmi S, Li Z, Dement AD, Cho KH, Kim JH. The glucose metabolite methylglyoxal inhibits expression of the glucose transporter genes by inactivating the cell surface glucose sensors Rgt2 and Snf3 in yeast. *Mol Biol Cell*. 2016;27(5):862-871. doi:10.1091/mbc.E15-11-0789
62. Stenina O. Regulation of Vascular Genes by Glucose. *Curr Pharm Des*. 2005;11(18):2367-2381. doi:10.2174/1381612054367283
63. Stitt AW. AGEs and diabetic retinopathy. *Investig Ophthalmol Vis Sci*. 2010;51(10):4867-4874. doi:10.1167/iovs.10-5881
64. Kim D-I, Lim S-K, Park M-J, Han H-J, Kim G-Y, Park SH. The involvement of phosphatidylinositol 3-kinase /Akt signaling in high glucose-induced downregulation of GLUT-1 expression in ARPE cells. *Life Sci*. 2007;80(7):626-632. doi:10.1016/J.LFS.2006.10.026
65. Dehdashtian E, Mehrzadi S, Yousefi B, et al. Diabetic retinopathy pathogenesis and the ameliorating effects of melatonin; involvement of autophagy, inflammation and oxidative stress. *Life Sci*. 2018;193:20-33. doi:10.1016/j.lfs.2017.12.001
66. Saxton RA, Sabatini DM. mTOR Signaling in Growth, Metabolism, and Disease. *Cell*. 2017;168(6):960-976. doi:10.1016/j.cell.2017.02.004
67. Harwood FC, Klein Geltink RI, O'Hara BP, et al. ETV7 is an essential component of a rapamycin-insensitive mTOR complex in cancer. *Sci Adv*. 2018;4(9). doi:10.1126/sciadv.aar3938
68. Wellen KE, Thompson CB. Cellular Metabolic Stress: Considering How Cells Respond to Nutrient Excess. *Mol Cell*. 2010;40(2):323-332. doi:10.1016/j.molcel.2010.10.004
69. Buller CL, Heilig CW, Brosius FC. GLUT1 enhances mTOR activity independently of TSC2 and AMPK. *Am J Physiol - Ren Physiol*. 2011;301(3):F588-F596. doi:10.1152/ajprenal.00472.2010
70. Lu L, Seidel CP, Iwase T, et al. Suppression of GLUT1; A new strategy to prevent diabetic complications. *J Cell Physiol*. 2013;228(2):251-257. doi:10.1002/jcp.24133
71. Wei J, Jiang H, Gao H, Wang G. Blocking Mammalian Target of Rapamycin (mTOR) Attenuates HIF-1α Pathways Engaged-Vascular Endothelial Growth Factor (VEGF) in Diabetic Retinopathy. *Cell Physiol Biochem*. 2016;40(6):1570-1577. doi:10.1159/000453207
72. Zhang MH, Jiang JZ, Cai YL, Piao LH, Jin Z. Significance of dynamic changes in gastric smooth muscle cell apoptosis, PI3K-AKT-mTOR and AMPK-mTOR signaling in a rat model of diabetic gastroparesis. *Mol Med Rep*. 2017;16(2):1530-1536. doi:10.3892/mmr.2017.6764

73. Ehrenkranz JRL, Lewis NG, Kahn CR, Roth J. Phlorizin: A review. *Diabetes Metab Res Rev*. 2005;21(1):31-38. doi:10.1002/dmrr.532
74. Shen L, You B an, Gao H qing, Li B ying, Yu F, Pei F. Effects of phlorizin on vascular complications in diabetes db/db mice. *Chin Med J (Engl)*. 2012;125(20):3692-3696. doi:10.3760/cma.j.issn.0366-6999.2012.20.017
75. Zhang S yang, Li B ying, Li X li, et al. Effects of phlorizin on diabetic retinopathy according to isobaric tags for relative and absolute quantification-based proteomics in db/db mice. *Mol Vis*. 2013;19:812-821.
76. Lechner J, O'Leary OE, Stitt AW. The pathology associated with diabetic retinopathy. *Vision Res*. 2017;139:7-14. doi:10.1016/j.visres.2017.04.003
77. Morita M, Gravel SP, Hulea L, et al. MTOR coordinates protein synthesis, mitochondrial activity. *Cell Cycle*. 2015;14(4):473-480. doi:10.4161/15384101.2014.991572
78. Alers S, Loffler AS, Wesselborg S, Stork B. Role of AMPK-mTOR-Ulk1/2 in the Regulation of Autophagy: Cross Talk, Shortcuts, and Feedbacks. *Mol Cell Biol*. 2012;32(1):2-11. doi:10.1128/mcb.06159-11
79. Fu D, Yu JY, Yang S, et al. Survival or death: a dual role for autophagy in stress-induced pericyte loss in diabetic retinopathy. *Diabetologia*. 2016;59(10):2251-2261. doi:10.1007/s00125-016-4058-5

Figures

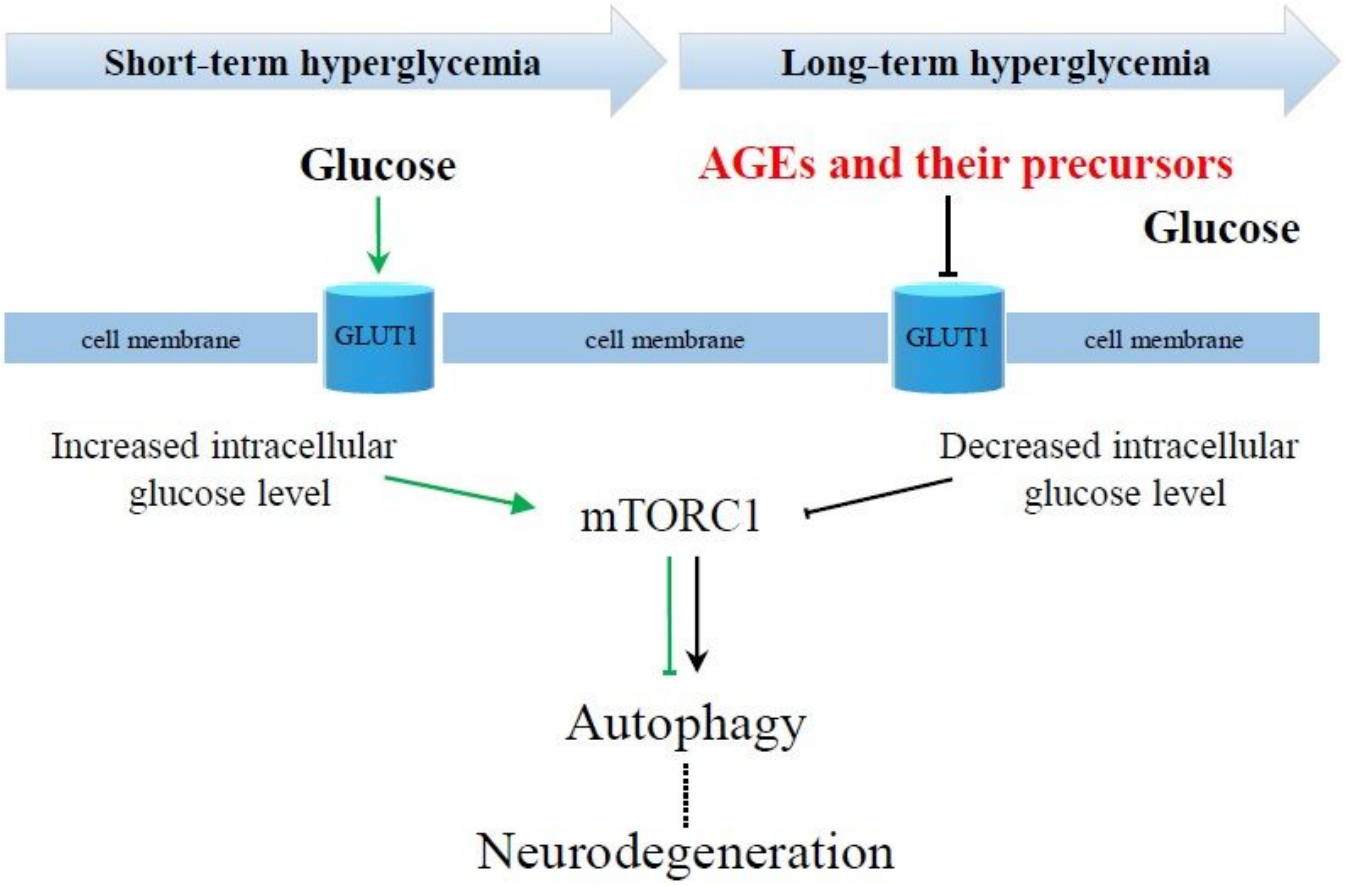

Figure 1

Schematic of the hypothesis. Schematic representation of mTORC1 activity regarding the duration of hyperglycemia. AGEs - advanced glycation end-products.

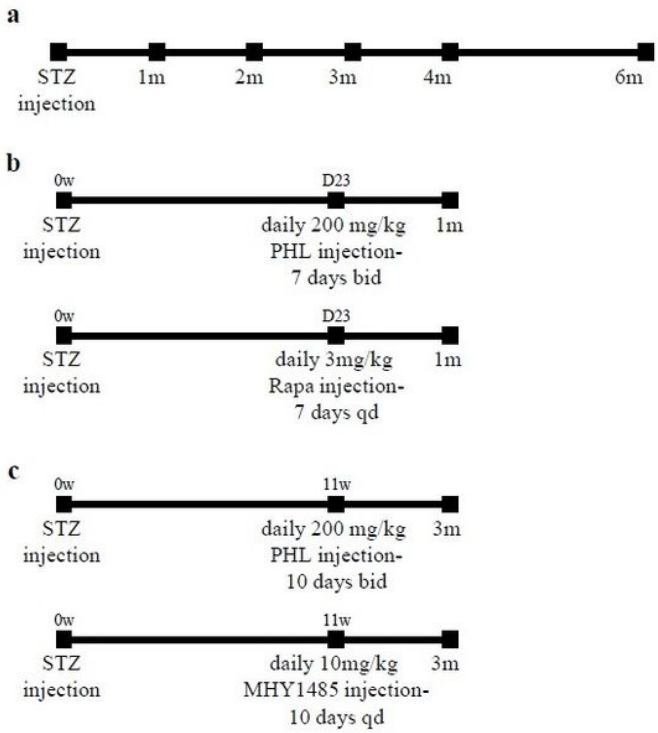

Table 1

Group		n	body weight (gr)	glucose level (mg/dL)
			mean±SD	mean±SD
a	**Normal**	10	30.5±1.2	161.9±14.1
	1 m DM	10	21.2±0.8	448±51.3
	2 m DM	10	24.8±1.2	458.7±67
	3 m DM	10	25.7±1.7	467.8±72.3
	4 m DM	9	28.5±2	500.5±71.1
	6 m DM	8	29±1.1	481.5±65.9
b	**Normal**	10	22.25±0.8	165.5±20.9
	1 m DM	10	21.05±0.7	488.6±63.8
	1 m DM/PHL	10	21.4±1.7	231.3±43.9
	1 m DM/Rapa	9	20.85±2.4	461.2±53.4
c	**Normal**	10	27.55±0.9	163±14.7
	3 m DM	9	25.6±1.5	466.7±71.8
	3 m DM/PHL	9	25.9±1.6	198±38.9
	3 m DM/MHY	8	24.8±1.2	470.7±73.1

Figure 2

Study design and general parameters of mice; bid – twice a day, qd – once a day. Table 1 Body weight and blood glucose level dynamics.

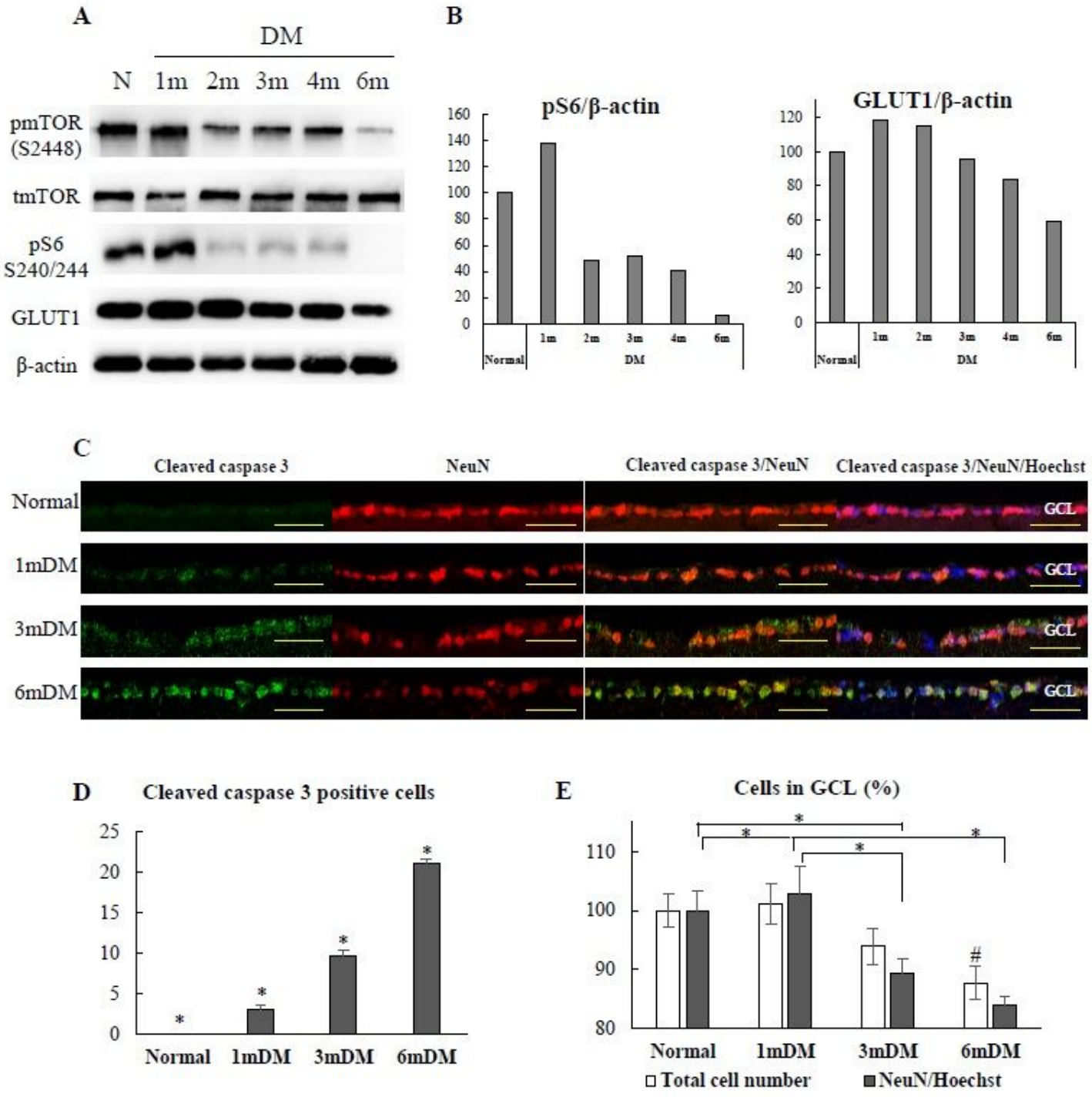

Figure 3

Hyperglycemia-induced molecular events and consequences in STZ mice retina. A – The expression of mTOR related proteins, GLUT1 and β-actin detected by Western blot. B – relative expression of the pS6 ribosomal protein and GLUT1 normalized to β-actin. C – cryosections of the mouse retina immunostained for cleaved caspase 3 (green) and NeuN (red), GCL – ganglion cell layer; Scale bar: 50μm. D – Cleaved caspase 3 positive cell number in the GCL of the normal and diabetic mouse retina (n=6/group). E – Total cell number and NeuN positive cell number (normalized to the Hoechst nuclear

counterstain) in the GCL of the normal and diabetic mouse retina. (n=6/group). # – P ≤ 0.05, compared with the Normal and 1mDM group; * – P ≤ 0.05.

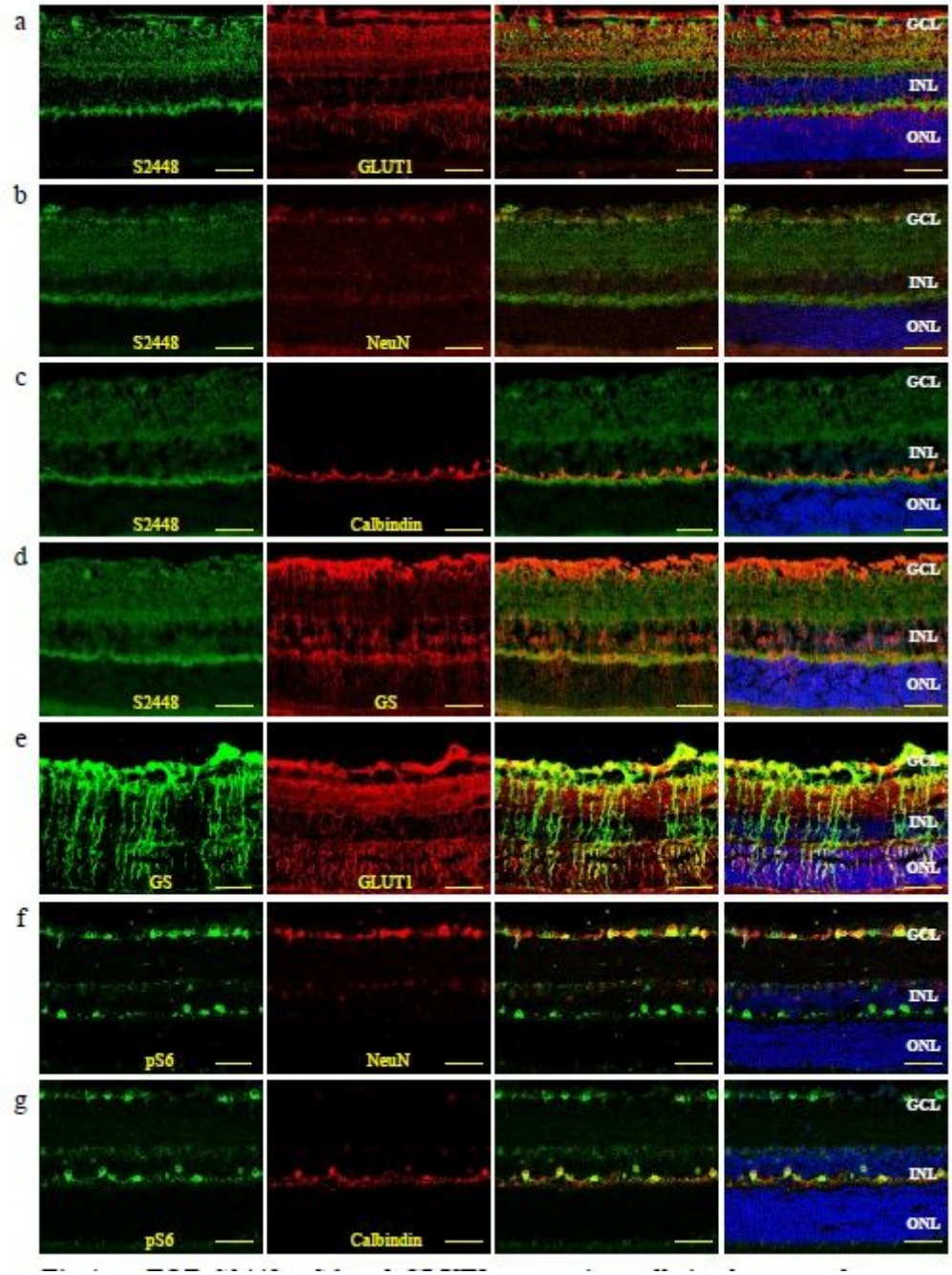

Figure 4

pmTOR S2448, pS6 and GLUT1 expressing cells in the normal mouse retina. Cryosections of normal mouse immuno-co-stained with pmTOR S2448 (green) and GLUT1 (red) (a), or NeuN (red) (b), or Calbindin (red) (c), or Glutamine synthetase (GS - red) (d), GS (green) and GLUT1 (red) (e), pS6 (green) and NeuN (red) (f), or Calbindin (red) (g). Nuclei were counter-stained with Hoechst 33342 (blue). GCL – ganglion cell layer; INL – inner nuclear layer; ONL – outer nuclear layer; Scale bar: 50μm

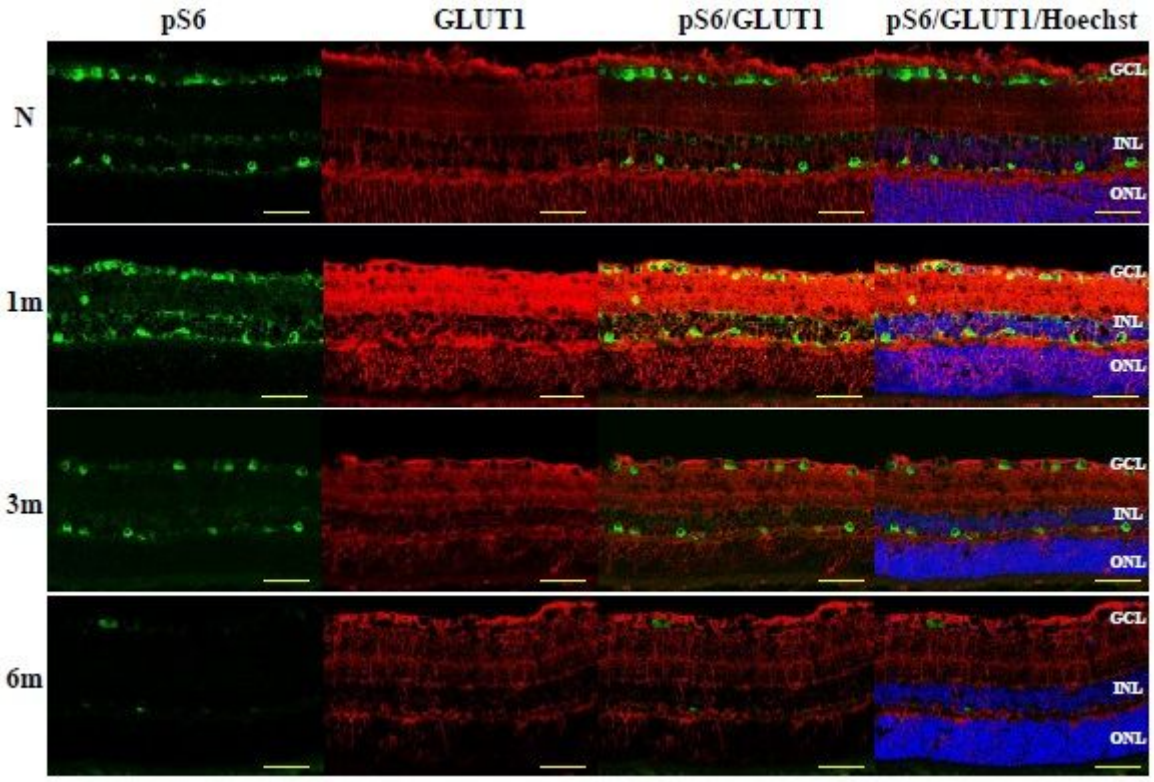

Figure 5

pS6 and GLUT1 expression dynamics over 6 months of observation of STZ-induced DM mice.

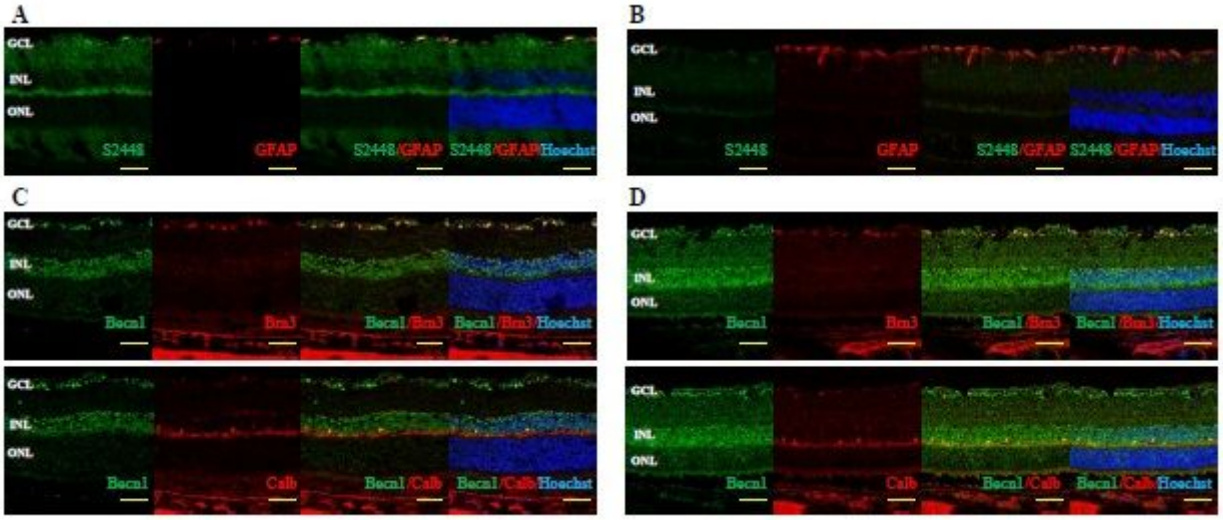

Figure 6

Autophagy and glia activation in the retina of STZ-induced DM. Immuno-co-staining for pmTOR S2448 (green) and GFAP (red) of normal (A) and 3 m DM mouse retina (B). Immuno-co-staining for Beclin1 (green) and Calbindin or Brn3 (red) of normal (C) and 3 m DM mouse retina (D). GCL – ganglion cell layer; INL – inner nuclear layer; ONL – outer nuclear layer; Scale bar: 50μm

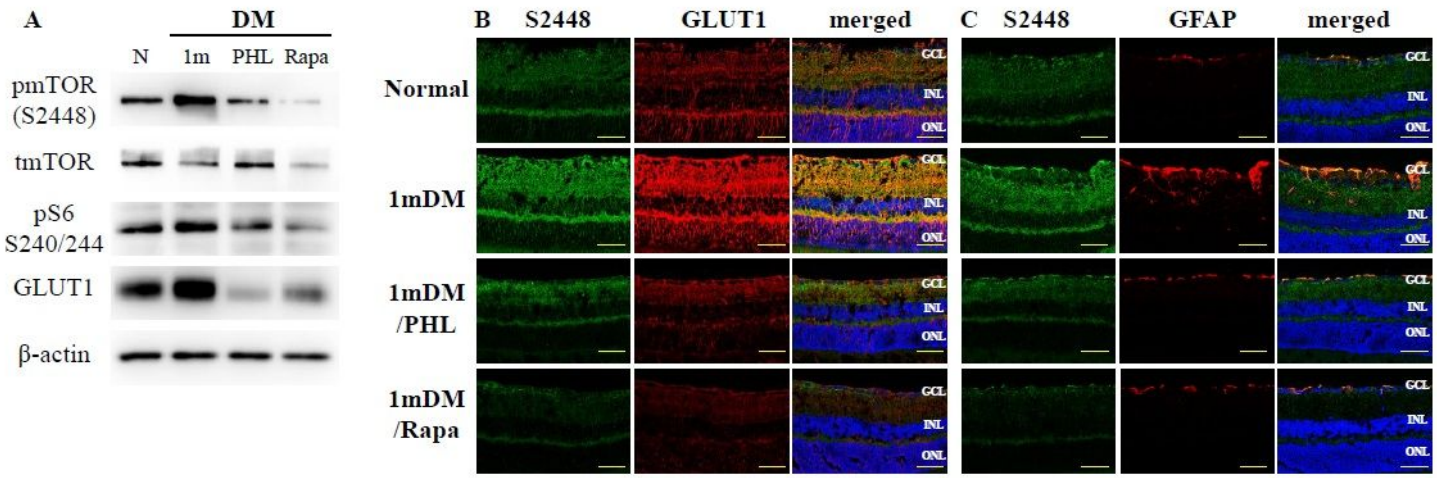

Figure 7

The effects of short-term hyperglycemia on STZ-mouse retina are reversible by glycemic control. A – The expression of mTOR related proteins, GLUT1 and β-actin detected by Western blot. B – Immuno-co-staining for pmTOR S2448 (green) and GLUT1 (red) of the retina from normal and 1-month diabetic mice treated with either phlorizin or rapamycin. C - Immuno-co-staining for pmTOR S2448 (green) and GFAP (red) of the retina from normal and 1-month diabetic mice treated with either phlorizin or rapamycin (A). Nuclei were counter-stained with Hoechst 33342 (blue). GCL – ganglion cell layer; INL – inner nuclear layer; ONL – outer nuclear layer; Scale bar: 50μm.

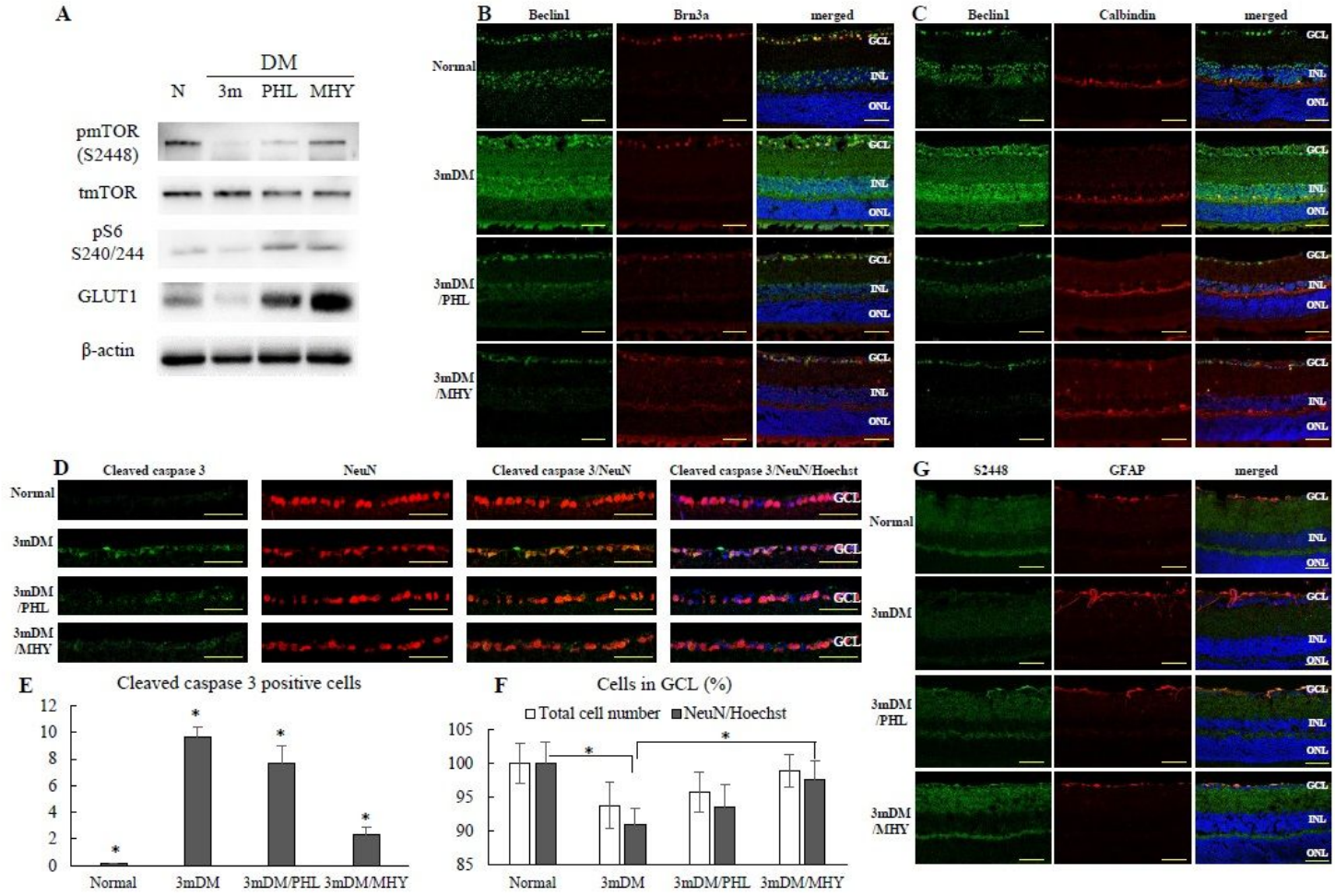

Figure 8

Autophagy dysregulation contributes to neuronal damage after long-term hyperglycemia. A – The expression of mTOR related proteins, GLUT1 and β-actin detected by Western blot. Immuno-co-staining for Beclin1 (green) and Brn3a (red) (B) or Calbindin (red) (C) of the retina from normal and 3-months diabetic mice treated with either phlorizin or MHY1485. D – Immuno-co-staining for Cleaved caspase 3 (green) and NeuN (red) of the retina from normal and 3-months diabetic mice treated with either phlorizin or MHY1485. E – Cleaved caspase 3 positive cell number in the retinal GCL of the indicated groups of mice (n=6/group). F – Total cell number and NeuN positive cell number (normalized to the Hoechst nuclear counterstain) in the retinal GCL of the indicated groups of mice (n=6/group). G – Immuno-co-staining for pmTOR S2448 (green) and GFAP (red) of the retina from normal and 3-months diabetic mice treated with either phlorizin or MHY1485. Nuclei were counter-stained with Hoechst 33342 (blue). GCL – ganglion cell layer; INL – inner nuclear layer; ONL – outer nuclear layer; * – $P \leq 0.05$; Scale bar: 50μm.

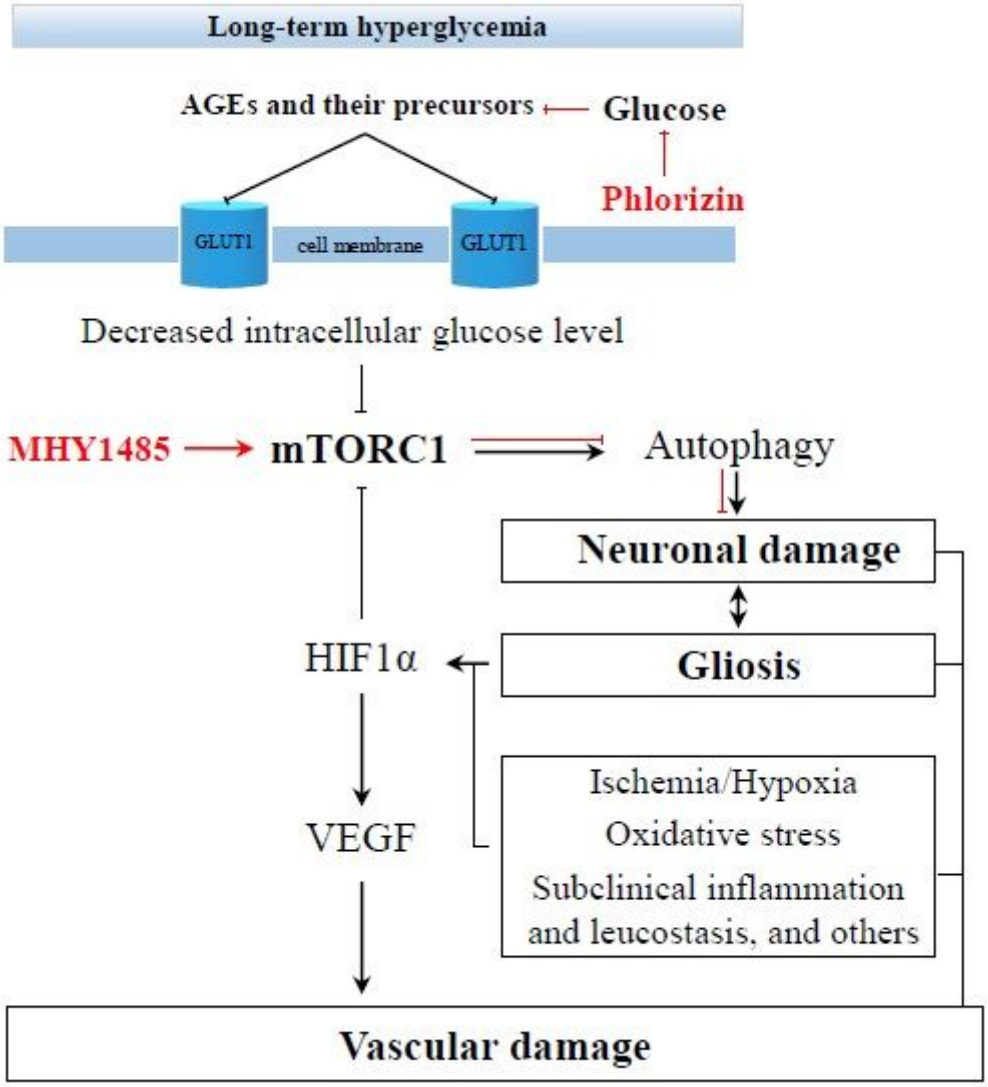

Figure 9

Schematic representation of the mechanism of neuronal cell rescue by autophagy modulation.

Supplementary Files

This is a list of supplementary files associated with this preprint. Click to download.

- Supplementalfigures.pdf